Diyala Journal of Engineering Sciences

Journal homepage: https://djes.info/index.php/djes

ISSN: 1999-8716 (Print); 2616-6909 (Online)

Optimizing Cancer Detection: Swarm Algorithms Combined with Deep Learning in Colon and Lung Cancer using Biomedical Images

HariKrishna Pathipati[1], Lova Naga Babu Ramisetti[2], Desidi Narsimha Reddy[3,*] Swetha Pesaru[4] Mashetty Balakrishna[5] and Thota Anitha[5]

[1]Department of Information Technology, ITG technologies, 10998 S Wilcrest Dr, Houston, TX 77099
[2]Department of Information Technology, Vignana Bharathi Institute of Technology, Aushapur, Hyderabad, India- 501301
[3]Data Consultant (Data Governance, Data Analytics: enterprise performance management, AI&ML), Soniks consulting LLC, USA
[4]Department of Information Technology, Vignana Bharathi Institute of Technology, Aushapur, Hyderabad, India- 501301
[5]Department of Computer science, Malla Reddy Engineering College

ARTICLE INFO

Article history:
Received August 22, 2024
Revised January 23, 2025
Accepted February 10, 2025
Available online March 1, 2025

Keywords:
Colon and lung cancer
Deep learning
Biomedical images
Whale optimization algorithm
Image preprocessing

ABSTRACT

Cancer is a deadly disorder, which affected by a mixture of genetic illnesses and a diversity of organic anomalies. Colon and lung cancer has been arisen as dual of the foremost origins of disability and death in humans. The histopathological recognition of such diseases is generally the most significant module in defining the finest progress of action. Prompt disease recognition on both front significantly reduces the probability of death. Machine learning (ML) and deep learning (DL) approaches are employed to haste up cancer recognition, letting researchers to analysis a great amount of patients in a short period of time and at a low cost. This research presents an Optimizing Cancer Detection using whale optimizer with Deep Learning in Colon and Lung Cancer (OCDWO-DLCLC) model on Biomedical Images. The presented OCDWO-DLCLC technique makes use of biomedical images for the recognition of colon and lung cancer. To achieve this, the OCDWO-DLCLC system uses wiener filtering (WF) technique for noise elimination process. In addition, the OCDWO-DLCLC technique uses NASNet Mobile model for learning complex feature patterns. Also, the hybrid of convolutional bidirectional gated recurrent unit (CNN-BiGRU) model was applied for classifying the existence of colon and lung cancer in the biomedical images. Eventually, the whale optimization algorithm (WOA) is used to optimally choose the hyperparameters of the CNN-BiGRU model. To confirm the improved analytical outcomes of the OCDWO-DLCLC approach, extensive simulations are executed on benchmark dataset. The comparative outcome analysis displays the promising performance of the OCDWO-DLCLC method on the recent models.

1. Introduction

Cancer occurs due to the unrestrained development of diseased cells within the body tissues or organs. Cancer cells might follow in distinct tissues or organs in body [1]. By 2020, Lung and Colon tumors have been predicted and categorized as the best 3 normal cancer types, according to a statistical analysis made in the US. Lung cancer is another cancer through a colon tumor [2]. Simply, the patient can be affected by either a lung or colon tumor concurrently. Hence, it can be active to test both cancer types and to identify them in advance. The usual signs are fatigue, muscle pain, cough, and so on followed by different types of diseases [3]. Most of the commonly utilized radiographic imaging approaches are mammography, ultrasound, computed tomography (CT), histopathological imaging, positron emission

* Corresponding author.
E-mail address: dn.narsimha@gmail.com
DOI: 10.24237/djes.2025.18105

tomography (PET), and magnetic resonance imaging (MRI) for cancer recognition [4]. Histopathological images are broadly utilized by health experts for diagnosis, and they are most significant in forecasting patients' survival probabilities. Conventionally, to identify cancer by investigative histopathological images, health experts have to go over a longer procedure; but, it is now possible to implement this method in less effort and time with the technical tools offered [5]. Therefore, it also requires a robust time-consuming, and focused task. Similarly, case recognition is complicated in the case of primary detection; the symptoms are vague and challenging to detect [6].

In recent times, artificial intelligence (AI) techniques have been identified for their capacity to study data quickly and in making decisions [7]. Similarly, in medical jobs, deep learning (DL) and machine learning (ML) are normally utilized techniques to analyze biological data. ML is a branch of AI techniques that are derived from the domain of cognitive acquisition and pattern detection models. It gives mechanisms that efficiently adapt over a huge set of information and create predictions depending on historical data [8]. During many sectors where emerging clear technologies with suitable efficacy appeared hard and practically impossible, ML has been effectively utilized with significant results [9]. On the other hand, DL is a complex pattern classification technique that has presented excellent outcomes in object recognition, voice detection, feature extraction, and other fields that need multi-level data handling. It can remove significant patterns from images and is established to get state efficacy, sometimes dominating humans [10].

This research presents an Optimizing Cancer Detection using a whale optimizer with Deep Learning in Colon and Lung Cancer (OCDWO-DLCLC) model on Biomedical Images. The presented OCDWO-DLCLC technique makes use of biomedical images for the recognition of colon and lung cancer. To achieve this, the OCDWO-DLCLC system uses the wiener filtering (WF) technique for the noise elimination process. In addition, the OCDWO-DLCLC technique uses the NASNetMobile model for learning complex feature patterns. Also, the hybrid of convolutional bidirectional gated recurrent unit (CNN-BiGRU) model was applied for classifying the existence of colon and lung cancer in biomedical images. Eventually, the whale optimization algorithm (WOA) is used to optimally choose the hyperparameters of the CNN-BiGRU model. To confirm the improved analytical outcomes of the OCDWO-DLCLC approach, extensive simulations are executed on benchmark dataset.

2. Related works

Kumar et al. [11] presented a comparative study of 2 feature extraction methods proposed for lung and colon cancer classifications. In one method, 6 customized feature extraction methods based on structure, shape, texture, and color are proposed. SVM-RBF, GB, RF, and MLP classifications with customized features have been tested and trained for the identification of lung and colon cancer. In the next method, utilizing the perception of TL, 7 DL methods for extracting the deep feature from lung and colon cancer HI are suggested. Anusha et al. [12] introduce a new method for lung and colon cancer diagnosis by utilizing VGG16 TL used for HI analysis. The author utilized the VGG16 CNN and leveraged TL to modify the model to the distinctive features of histopathological imaging. The study complicated difficult pre-processing to enhance and standardize the quality of the image, and assuring the VGG16 method can efficiently differentiate and learn different tissue patterns. Kumar et al. [13] presented a less complex and lightweight CNN-based structure for automatic identification of multiclass colorectal tissue HI by employing 2 freely accessible datasets, NCT-CRC-HE-100K, and colorectal histology, correspondingly. HI is offered as input to pre-trained methods VGG16, InceptionResNetV2, DenseNet121, Xception, and the presented system colorectal cancer classification CNN. This is the initial research, which equates the computing time of various DL structures for the colorectal tissue classification. The advanced system needs less computing time for training related to another pre-trained method.

Peng and Wu [14] presented a dataset that contains HI of lung and colon cancer from

Kaggle. The data contained 5 separate classifications of the lung and colon tissues. To categorize the images, the author utilized a DL method that used pretrained NN called AlexNet. Afterward tuning the presented method by replacing the preceding FC layer, SGDM optimizers are used to enhance the parameters. Tsai et al. [15] introduce a MOMA platform, an explainable ML method, to constantly interpret and identify the relationship among patients', multi-omics, clinical profiles, and histologic patterns in 3 huge patient cohorts (n = 1888). Furthermore, our methods classify interpretable pathology patterns analytical of microsatellite uncertainty condition, clinically actionable genetic, and changes in gene expression profiles. The MOMA methods have been generalizable to many patient populations with various demographic pathology images and compositions gathered from distinct digitization techniques. ML methods offer clinically actionable predictions, which can advise treatments for colorectal cancer patients.

Pasha and Narayana [16] presented DL and ML methods that are used to accelerate the recognition cancer process that can also assist the investigators in learning a vast number of patients across a less loss and short period. Therefore, it is greatly important to make a novel lung and colon recognition method based on DL methods. At first, a various group of HI is gathered from benchmark sources to execute an effectual study. Later, to achieve the initial features group, the gathered image is provided to the expanded net for achieving deep image features with the aid of ResNet and VGG16. Shanmugam and Rajaguru [17] present a new technique for the recognition of lung cancer utilizing HI. In this study, the HI experienced pre-processing, succeeded by segmentation by utilizing a segmented image intensity, and the adapted method of KFCM-based segmentation values are reduced dimensionally by utilizing the GWO and PSO.

3. Methodology

In this research, we have presented a new OCDWO-DLC model on Biomedical Images. The presented OCDWO-DLCLC technique makes use of biomedical images for the identification of colon and lung cancer. Figure 1 represents the entire procedure of the OCDWO-DLCLC model.

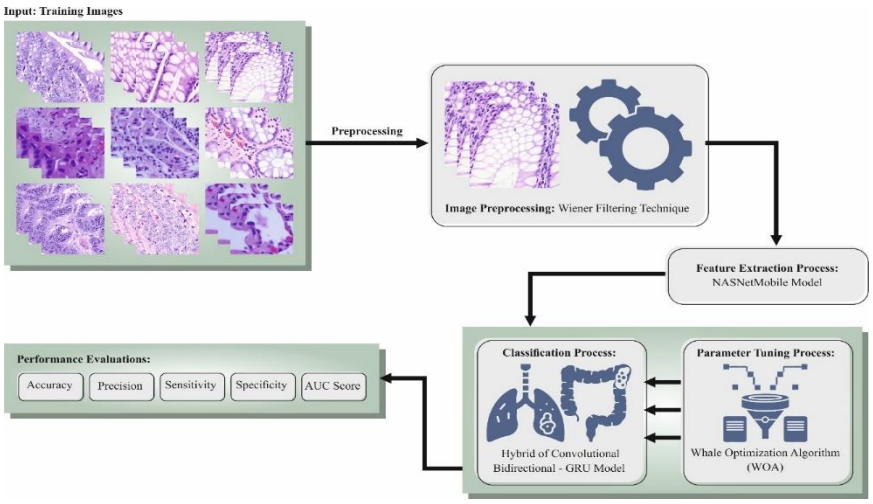

Figure 1. Overall process of OCDWO-DLCLC model

3.1. Image preprocessing

Primarily, the OCDWO-DLCLC system uses the WF technique for the noise elimination process. WF is a great image preprocessing model employed in biomedical imaging to improve the excellence of images, mainly for lung and colon cancer recognition [18]. By estimating and decreasing noise in the images, WF enhances the detail and clarity of crucial features, helping in the precise classification of tumorous tissues. This approach alters the filter

depending on the local variance of the image, maintaining significant edges while smoothing out noise. In lung and colon cancer recognition, WF aids in making more reliable and clearer images for enhanced analysis and diagnosis.

3.2. Feature extraction

In addition, the OCDWO-DLCLC technique uses the NASNetMobile model for learning complex feature patterns. NAS is a technique, which automatizes the growth of NN structure to obtain the finest outcomes on a particular task [19]. The aim is to generate the framework employing as limited sources and as few human interruptions as possible. The NasNet structure is a neural framework searching network that is trained to get the best accurate parameters from the created architecture using reinforcement learning and Recurrent NN (RNN). Inventing a CNN architecture continues for a while after the data is enormous like the Image Net dataset. Then we generated a CNN architecture that can find the optimum structure in a smaller data quantity and then transfer that framework to be trained in a larger dataset; these frameworks can be considered "learning transferable architectures". This NasNet-Mobile framework is scaled based on the size of the data.

The NasNet-Mobile architecture is constructed on depth-wise distinguishable convolutions, a factored convolution type in which a normal convolution can be separated into depth wise convolution and a 1x1 convolution expressed as a point wise convolution. The NasNet-Mobile utilizes depth-wise convolution for applying distinct filters to every input network. This point-wise convolution then executes a 1x1 convolution of the depth-wise convolution outputs. The classic convolution model mixes and filters inputs in a solitary stage to create a novel collection of outputs. The depth-wise discrete convolution distributes this into dual layers: combining and filtering. The factorization significantly reduces the model and processing dimension. Depth-wise divisible convolutions are made up of dual layers: depth-wise and point-wise. They use depth wise convolutions (depth of input) to generate a solitary filter for every input channel. In the depth wise layer, the output can be formerly linearly joined with a point-wise convolution that can be a simple 1x1 convolution Eq. (1).

$$G_{k,l,m} = \sum_{i,j} \hat{k}_{i,j} * F_{k+i-1}, i + j - 1, m \quad (1)$$

Now, K represents a depth wise convolutional kernel with a dimension of DkxDkxM whereas m^th filter in kˆ has been utilized for the m^th channel in F to output the m^th filter output channel featured mapping G. Figure 2 illustrates the architecture of NASNetMobile.

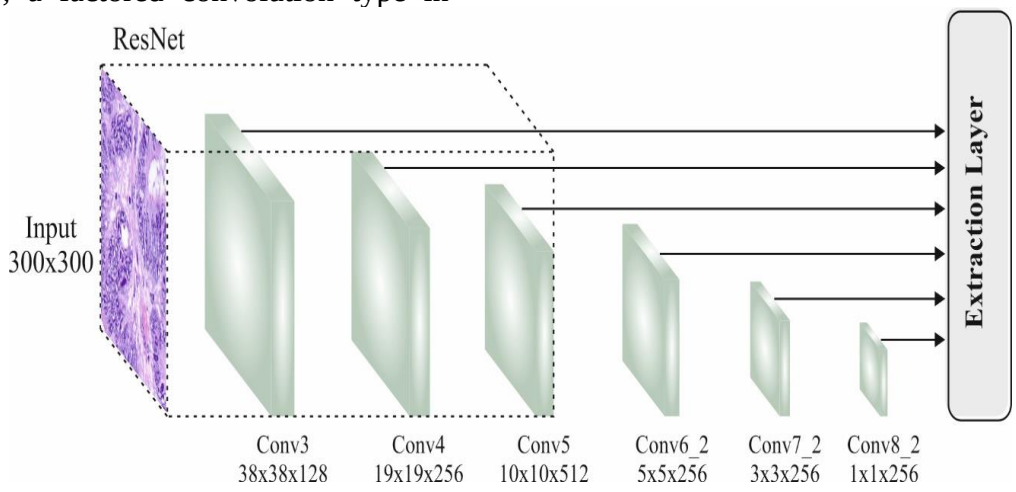

Figure 2. Structure of NASNetMobile

3.3. Hybrid of CNN-BiGRU Model

In this phase, the CNN-BiGRU hybrid method has been applied to classify existence of colon and lung cancer in the biomedical images. The hybrid of CNN-BiGRU structure in the analysis integrates 1D CNN layers and BiGRU dual layers for modeling the regression [20]. It permits the dataset of input transfer over BiGRU and CNN and, therefore uses the advantages of both platforms in the data process for training the hybrid method. Therefore, it controls the powers of both frameworks for processing serial datasets. It gets the better CNN capacity for feature extraction after which permits the BiGRU to take serial dependency. The fine-tuning of parameters can be performed with grid search in Python. The search of grid contains hyperparameters for the hybrid approach during the optimization of parameters, which offer the finest values like dropout, regularization of weight, and batch. Therefore, a hybrid CNN-BiGRU technique holds the benefit of using the abilities of BiGRU and CNN DL structure.

CNN is a backward and feedforward neural network (FFNN), which is examined to operate in dual segments: classification and feature extraction. CNN is dissimilar to a standard NN by addition of various layers, sharing of weights, local connections, and pooling. BiGRU is DL architecture with two GRUs. Hence, the CNN-BiGRU system can effectively capture time-based dependency in data and utilizes these dual gate methods to discriminatively upgrade the hidden layer (HL) of the system at every stage, creating it an efficient device for prediction. It contains an update and reset gate that have the succeeding Eqs:

$$Update\ gate: z = \delta(W_z h_{t-1} + U_z x_t) \quad (2)$$

$$Reset\ gate: r = \delta(W_r h_{t-1} + U_r x_t) \quad (3)$$

The GRU require dual inputs, a prior state of cell (h_{t-1}) and input of training data (x_t), resultant in output of cell (h_t). This can be distributed over the GRU unit subsequent parts:

× :Elementwise multiplication; +:Vector addition; Δ:Sigmoid function; Tanh:Hyper tangent function.

These analyses applied BiGRU that captures input in both backward and forward methods. These aids to improve its effectiveness for taking significant information from the input dataset.

3.4. Hyperparameter Selection

Eventually, the WOA is employed to optimally choose the hyperparameters of the CNN-BiGRU model. Mirjalili and Lewis 2016 introduced WOA, a heuristic optimization technique based on the hunting behavior of humpback whales, which was mathematically modeled by simulating the attacking strategy of bubble net foraging and the behavior of the whales' round-up to accomplish optimization [21]. The VVOA has the benefits of an effectual global search ability, a small quantity of control parameters, and uncomplicated implementation. This follows a three-stage process that simulates the feeding behavior and typical search method of humpback whales: prey searching, prey seining, and bubble net foraging. The WOA studies each humpback whales position as a promising solutions, and the optimum solution can be attained by continuously reviewing whale's locations in the solution space.

1. Rounding up prey

WOA assumes the best candidate solution can also be the preferred victim or a solution closer to optimum. Once finding the optimum agent of search, the succeeding search agent strives to match the position with the superior agent. The succeeding formula expresses these behaviors.

$$\vec{D} = \left|\vec{C} \cdot \vec{X^*}(t) - \vec{X}(t)\right| \quad (4)$$

$$\vec{X}(t+1) = \vec{X^*}(t) - \vec{A} \cdot \vec{D} \quad (5)$$

Here t indicates the existing iteration number, and the coefficient vectors are A $\vec{}$ and C $\vec{}$. The location vector X $\vec{}$*(t) denotes the better solution obtained thus far. The update of X $\vec{}$*(t) will be made on each iteration once the better solution is available.

$$\vec{A} = 2\vec{a} \cdot \vec{r_1} - \vec{a} \quad (6)$$

$$\vec{C} = 2 \cdot \vec{r_2} \quad (7)$$

$$\vec{a} = 2 - \frac{2t}{T_{\max}} \quad (8)$$

Where $\vec{a}$ is linearly dropped from 2 to 0 at the iterative method, and $\overrightarrow{r_1}$ and $\overrightarrow{r_2}$ are random vectors within [0,1]. T_{max}denotes the maximal iteration counter.

2. Bubble Netting

The predation of Humpback whales chiefly takes place through encircling and bubble-net predation. Using the subsequent formula, the humpback whales and prey location updates during bubble-net feeding are computed.

$$\vec{X}(t+1) = \vec{D}' \cdot e^{bt} \cdot \cos(2\pi l) + \vec{X} * (t) \quad (9)$$

$$\vec{D}' = \left|\vec{X} * (t) - \vec{X}(t)\right| \quad (10)$$

Here D $\vec{}$' refers to the distance vector between the present optimal solution and the present searching individual, b is a finite constant defining the helix shape, and l is a uniformly and randomly distributed value within [-1, 1].

The WOA shows the two predatory behaviors: bubble-net predation or constriction encirclement while leaning towards the prey. p defines the choice between those behaviors and the location is updated by the following equation:

$$\vec{X}(t+1) = \begin{cases} \vec{X} * (t) - \vec{A} \cdot \vec{D}, p < 0.5, \\ \vec{D}' \cdot e^{bl} \cdot \cos(2\pi l) + \vec{X} * (t), p \geq 0.5. \end{cases} \quad (11)$$

In Eq. (11), p is the probability of the predation mechanism, a random value between [0,1].

A gradual reduction takes place in the parameter $\vec{A}$ and the convergence factor a following an increase in iterations t, and when $\left|\vec{A}\right| < 1$, then whales gradually enclose the present optimum solution as a part of XVOA's local optimum search space.

3. Searching for prey

WOA adjusts the whale's position based on the distance from other whales to enable detailed exploration of the solution space, thereby promoting random searching. When $|\vec{A}| \geq 1$, then the individuals swim towards random whales:

$$\vec{D} = \left|\vec{C} \cdot \vec{X}(t) - \vec{X}(t)\right| \quad (12)$$

$$\vec{X}(t+1) = \vec{X}(t) - \vec{A} \cdot \vec{D} \quad (13)$$

Here $\vec{D}$ indicates the distance separating the random individuals from the present search individuals, $\vec{X}_r(t)$ is the location vector of the existing individuals.

The WOA provides various benefits such as fewer parameters to tune, simplicity in implementation than other optimization techniques, and stronger global search ability. During the optimization process, it effectively balances exploration and exploitation, which makes it fit for resolving high-dimensional and complex optimization problems. Furthermore, WOA has illustrated efficiency and robustness in searching near-optimal or optimal solutions throughout different applications.

On the other hand, WOA has certain drawbacks: (1) The WOA performance can be influenced highly by the parameters including the step size, direction, initial location of the whale, etc. Such parameters considerably affect the algorithm efficacy. Insufficient parameter selection may lead to convergence towards the local optima or even suboptimal performance. (2) The WOA is a computing technique, which imitates the foraging behavior of whales to search for the optimum solution. This can be achieved by modeling the feeding behavior of whales. However, the method may get stuck in the local optimal solution whereas finding without searching for the global optimum solution owing to the whale's behaviour randomness. (3) The WOA shows a meaningful dependence on first solution. If the first solution is not properly selected, then it can adversely affect the search effectiveness and results of the algorithms.

The fitness selection is the significant factor impacting the performances of the WOA. The hyperparameter chosen process contains the solution encoding technique to assess the efficacay of the candidate solutions. In this study, the WOA studies precision as the main

criterion to form the fitness function (FF) that is stated below.

$$Fitness = \max(P) \quad (14)$$

$$P = \frac{TP}{TP + FP} \quad (15)$$

From the expression, TP and FP represents the true positive and false positive value.

4. Experimental results and analysis

The performance validation analysis of OCDWO-DLCLC model using benchmark dataset [22]. It holds 25000 samples with five class labels are represented in Table 1.

Table 1: Details on dataset

Class Names	Labels	No. of Images
"Lung benign tissue"	Lung-C1	5000
"Lung adenocarcinoma"	Lung-C2	5000
"Lung squamous cell carcinoma"	Lung-C3	5000
"Colon adenocarcinoma"	Colon-C1	5000
"Colon benign tissue"	Colon-C2	5000
Total No. of Images		**25000**

Figure. 3 represents the classification results of the OCDWO-DLCLC process on the test dataset. Figures 3a-3b display the confusion matrix with precise identification and classification of all 5 class labels on a 70%:30% TRAP/TESP. Figure 3c shows the PR analysis, demonstrating maximum performance across all classes. Lastly, Figure 3d indicated the ROC analysis, representing efficient results with high ROC values for distinct class labels.

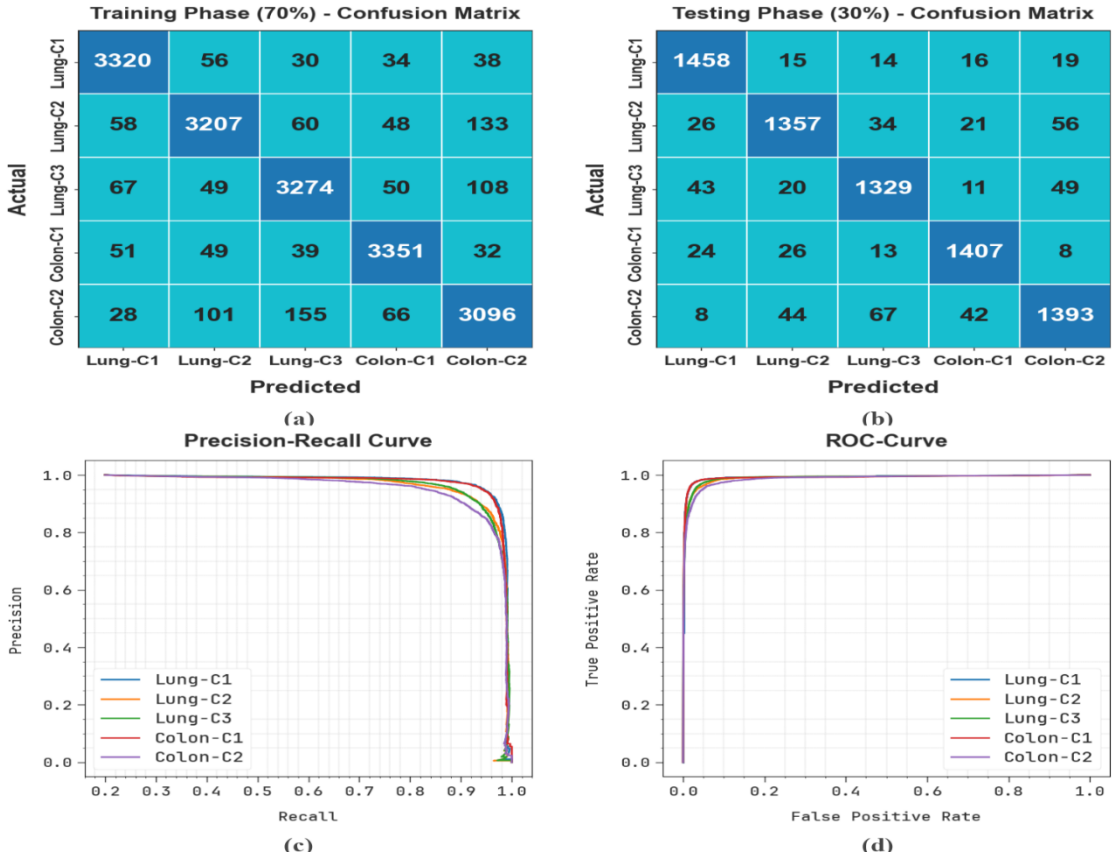

Figure 3. Classifier results of (a-b) Confusion matrices and (c-d) Curves of PR and ROC

In Table 2, the cancer recognition results of OCDWO-DLCLC model under 70%TRAP and 30%TESP are depicted. The table values implied that the OCDWO-DLCLC approach has properly identified five class labels. With 70%TRAP, the OCDWO-DLCLC technique offers average $accu_y$ of 97.14%, $prec_n$ of 92.83%, $sens_y$ of 92.84%, $spec_y$ of 98.21%, and AUC_{score} of 95.53%. Followed by, with 30%TESP, the OCDWO-DLCLC process provides an average $accu_y$ of 97.03%, $prec_n$ of 92.58%, $sens_y$ of 92.60%, $spec_y$ of 98.15%, and AUC_{score} of 95.37%.

Table 2: Cancer Detection outcome of OCDWO-DLCLC model under 70%TRAP and 30%TESP

Class Labels	$Accu_y$	$Prec_n$	$Sens_y$	$Spec_y$	AUC_{Score}
TRAP (70%)					
Lung-C1	97.93	94.21	95.46	98.55	97.00
Lung-C2	96.83	92.63	91.47	98.18	94.82
Lung-C3	96.81	92.02	92.28	97.96	95.12
Colon-C1	97.89	94.42	95.14	98.58	96.86
Colon-C2	96.22	90.87	89.84	97.79	93.82
Average	**97.14**	**92.83**	**92.84**	**98.21**	**95.53**
TESP (30%)					
Lung-C1	97.80	93.52	95.80	98.31	97.05
Lung-C2	96.77	92.82	90.83	98.25	94.54
Lung-C3	96.65	91.21	91.53	97.88	94.71
Colon-C1	97.85	93.99	95.20	98.51	96.85
Colon-C2	96.09	91.34	89.64	97.78	93.71
Average	**97.03**	**92.58**	**92.60**	**98.15**	**95.37**

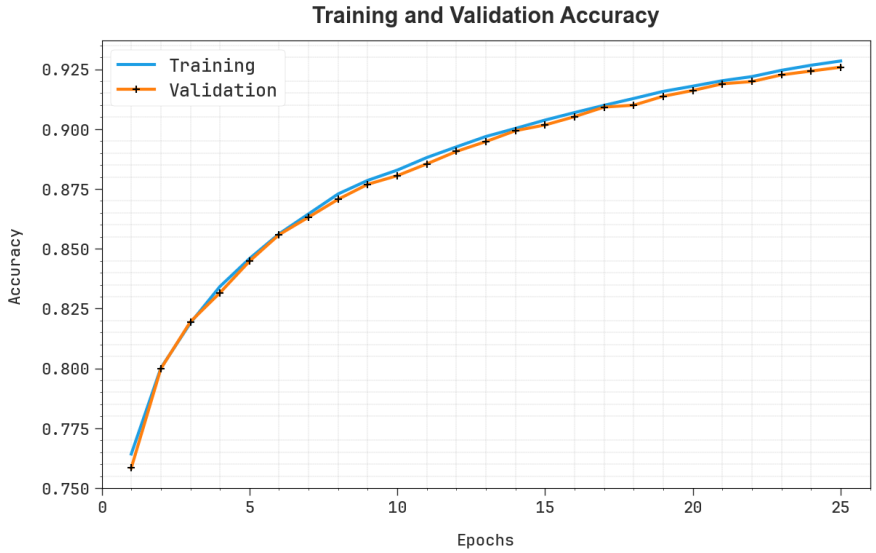

Figure 4. $Accu_y$ curve of the OCDWO-DLCLC model

In Figure 4, the training and validation accuracy outcomes of the OCDWO-DLCLC system are illustrated. The accuracy values are computed over an interval of 0-25 number of epochs. The figure emphasized that the training and validation accuracy values show a rising trend which notified the capability of the OCDWO-DLCLC method with improved performance over several iterations. Moreover, the training and validation accuracy remains closer over the epochs, which specifies low minimal overfitting and displays the enhanced performance of the OCDWO-DLCLC process, guaranteeing consistent prediction on unseen samples.

In Figure 5, the training loss and validation loss graph of the OCDWO-DLCLC system is shown. The loss values are computed over an interval of 0-25 epochs. It is depicted that the training and validation accuracy values showed a reducing trend, which notified the capability of the OCDWO-DLCLC process in balancing a trade-off between data fitting and generalization. The continual reduction in loss values additionally guarantees the enhanced performance of the OCDWO-DLCLC approach and tune the prediction results over time.

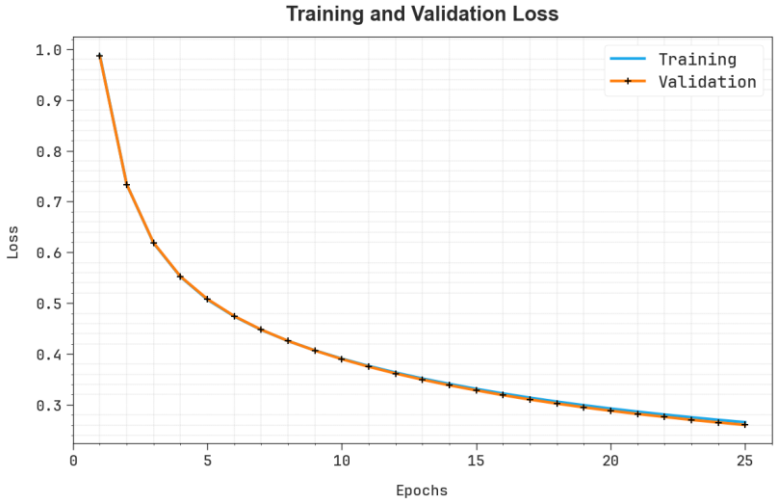

Figure 5. Loss curve of the OCDWO-DLCLC model

In Table 3 and Figure 6, the experimental results of the OCDWO-DLCLC process with recent models are given [23, 24]. The results display that the CapsNet process has shown worse performance with $Accu_y$ of 92.51%. At the same time, the REsNet50 and HDCAAPSL methods have attained slightly increased results with $Accu_y$ of 92.67% and 93.04%, correspondingly. Besides, the CNN+2D FT, DLCC-DLCF, and CNN+PCA approaches have obtained moderately closer performance with $Accu_y$ of 95.85%, 96.33%, and 96.51%, respectively. Meanwhile, the U-Net-CGPCHI process has resulted in considerable outcomes with $Accu_y$of 96.84%. But the OCDWO-DLCLC approach outperforms the other models with maximum $Accu_y$of 97.14%.

Table 3: $Accu_y$ outcome of OCDWO-DLCLC technique with recent models

Method	Accuracy %
OCDWO-DLCLC	97.14
U-Net-CGPCHI	96.84
CNN+PCA	96.51
DLCC-DLCF	96.33
CNN+2D FT	95.85
HDCAAPSL	93.04
ResNet50 Model	92.97
Capsule Network	92.51

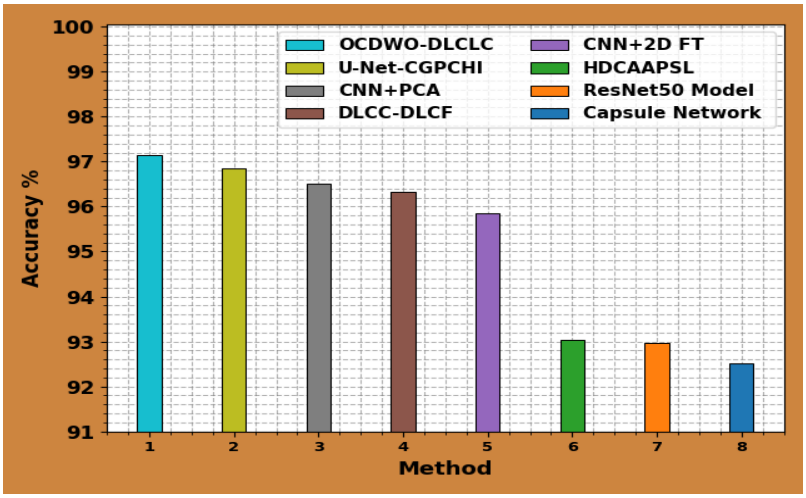

Figure 6. $Accu_y$ outcome of OCDWO-DLCLC technique with recent models

In Table 4 and Figure 7, the computational time (CT) results of the OCDWO-DLCLC method with recent models are given. The results display that the DLCC-DLCF system has shown worse performance with CT of 9.56s. At the same time, the CNN+2D FT and CapsNet process have attained slightly lesser outcomes with CT of 8.26s and 8.66s, correspondingly. Besides, the U-Net-CGPCHI, HDCAAPSL, and CNN+PCA approaches have obtained moderately closer performance with CT of 7.82s, 7.42s, and 7.84s, correspondingly. Meanwhile, the ResNet50 method has resulted in considerable outcomes with CT of 6.51s. However, the OCDWO-DLCLC model outperforms the other models with lesser CT of 4.67s.

Table 4: CT outcome of OCDWO-DLCLC technique with recent models

Method	Computational Time (sec)
OCDWO-DLCLC	4.67
U-Net-CGPCHI	7.82
CNN+PCA	7.84
DLCC-DLCF	9.56
CNN+2D FT	8.26
HDCAAPSL	7.42
ResNet50 Model	6.51
Capsule Network	8.66

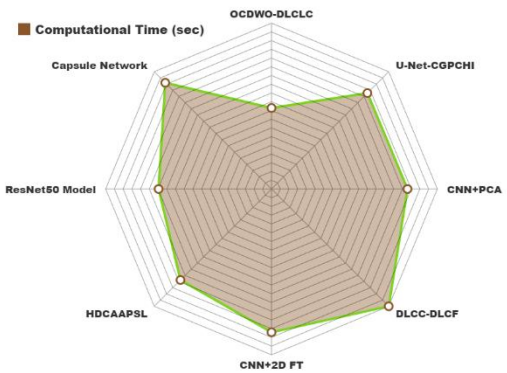

Figure 7. CT outcome of OCDWO-DLCLC technique with recent models

5. Conclusion

In this research, we have presented a new OCDWO-DLC model on Biomedical Images. The presented OCDWO-DLCLC technique makes use of biomedical images for the classification of colon and lung cancer. Primarily, the OCDWO-DLCLC system uses WF technique for the noise elimination process. In addition, the OCDWO-DLCLC technique uses the NASNetMobile model for learning complex feature patterns. Also, the hybrid of the CNN-BiGRU method was applied to classify the existence of colon and lung cancer in biomedical images. Eventually, the WOA is employed to optimally choose the hyperparameters of the CNN-BiGRU method. To confirm the improved analytical outcomes of the OCDWO-DLCLC approach, extensive simulations are executed on benchmark dataset. The comparative outcome analysis displays the promising performance of the OCDWO-DLCLC method on the recent models.

References

[1] Y. Zhuang, S. Chen, N. Jiang, and H. Hu, ‘‘An effective WSSENet-based similarity retrieval method of large lung CT image databases,’’ KSII Trans. Internet Inf. Syst., vol. 16, no. 7, 2022.

[2] R. R. Wahid, C. Nisa, R. P. Amaliyah, and E. Y. Puspaningrum, ‘‘Lung and colon cancer detection with convolutional neural networks on histopathological images,’’ Proc. AIP Conf. Proc., vol. 2654, no. 1, Feb. 2023.

[3] G. Yu, K. Sun, C. Xu, X.-H. Shi, C. Wu, T. Xie, R.-Q. Meng, X.-H. Meng, K.-S. Wang, H.-M. Xiao, and H.-W. Deng, ‘‘Accurate recognition of colorectal cancer with semi-supervised deep learning on pathological images,’’ Nature Commun., vol. 12, no. 1, p. 6311, Nov. 2021.

[4] L. Sun, M. Zhang, B. Wang, and P. Tiwari, ‘‘Few-shot class-incremental learning for medical time series classification,’’ IEEE J. Biomed. Health Informat., pp. 1–11, 2023.

[5] B. K. Hatuwal and H. C. Thapa, ‘‘Lung cancer detection using convolutional neural network on histopathological images,’’ Int. J. Comput. Trends Technol., vol. 68, no. 10, pp. 21–24, Oct. 2020.

[6] X. Xiao, Z. Wang, Y. Kong, and H. Lu, ‘‘Deep learning-based morphological feature analysis and the prognostic association study in colon adenocarcinoma histopathological images,’’ Frontiers Oncol., vol. 13, Feb. 2023, Art. no. 1081529.

[7] S. Mangal, A. Chaurasia, and A. Khajanchi, ‘‘Convolution neural networks for diagnosing colon and lung cancer histopathological images,’’ 2020, arXiv:2009.03878.

[8] O. Stephen and M. Sain, ‘‘Using deep learning with Bayesian–Gaussian inspired convolutional neural architectural search for cancer recognition and classification from histopathological image frames,’’ J. Healthcare Eng., vol. 2023, pp. 1–9, Feb. 2023.

[9] R. D. Mohalder, J. P. Sarkar, K. A. Hossain, L. Paul, and M. Raihan, ‘‘A deep learning based approach to predict lung cancer from histopathological images,’’ in Proc. Int. Conf. Electron., Commun. Inf. Technol. (ICECIT), Sep. 2021, pp. 1–4.

[10] D. Z. Karim and T. A. Bushra, ‘‘Detecting lung cancer from histopathological images using convolution neural network,’’ in Proc. IEEE Region Conf. (TENCON), Dec. 2021, pp. 626–631.

[11] Kumar, N., Sharma, M., Singh, V.P., Madan, C. and Mehandia, S., 2022. An empirical study of handcrafted and dense feature extraction techniques for lung and colon cancer classification from histopathological images. *Biomedical Signal Processing and Control*, *75*, p.103596.

[12] Anusha, M. and Reddy, D.S., 2024, March. Enhancing Lung and Colon Cancer Diagnosis: An ImageNet-Trained Transfer Learning Approach for Histopathological Image Analysis. In *2024 Tenth International Conference on Bio Signals, Images, and Instrumentation (ICBSII)* (pp. 1-4). IEEE.

[13] Kumar, A., Vishwakarma, A. and Bajaj, V., 2023. Crccn-net: Automated framework for classification of colorectal tissue using histopathological images. *Biomedical Signal Processing and Control*, *79*, p.104172.

[14] Peng, C.C. and Wu, J.W., 2023, June. Deep Learning-Assisted Lung Cancer Diagnosis from Histopathology Images. In *2023 IEEE 5th Eurasia Conference on Biomedical Engineering, Healthcare and Sustainability (ECBIOS)* (pp. 17-20). IEEE.

[15] Tsai, P.C., Lee, T.H., Kuo, K.C., Su, F.Y., Lee, T.L.M., Marostica, E., Ugai, T., Zhao, M., Lau, M.C., Väyrynen, J.P. and Giannakis, M., 2023. Histopathology images predict multi-omics aberrations and prognoses in colorectal cancer patients. *Nature communications*, *14*(1), p.2102.

[16] Pasha, M.A. and Narayana, M., 2023. Development of Trio Optimal Feature Extraction Model for Attention-Based Adaptive Weighted RNN-Based Lung and Colon Cancer Detection Framework Using Histopathological Images. *International Journal of Image and Graphics*, p.2550027.

[17] Shanmugam, K. and Rajaguru, H., 2023. Exploration and enhancement of classifiers in the detection of lung cancer from histopathological images. *Diagnostics*, *13*(20), p.3289

[18] Stanciu, C.L., Benesty, J., Paleologu, C., Costea, R.L., Dogariu, L.M. and Ciochină, S., 2023. Decomposition-based wiener filter using the Kronecker product and conjugate gradient method. *IEEE/ACM Transactions on Audio, Speech, and Language Processing*.

[19] KATEB, Y., EGLOULI, H. and AGUIB, S., 2024. Classifying Surface Fault in Steel Strips Using a Customized NasNet-Mobile CNN and Small Dataset. *J. Electrical Systems*, *20*(1), pp.52-67.

[20] Raj, N., Murali, J., Singh-Peterson, L. and Downs, N., 2024. Prediction of Sea Level Using Double Data Decomposition and Hybrid Deep Learning Model for Northern Territory, Australia. *Mathematics*, *12*(15), p.2376.

[21] Dai, L. and Wang, H., 2024. An Improved WOA (Whale Optimization Algorithm)-Based CNN-BIGRU-CBAM Model and Its Application to Short-Term Power Load Forecasting. *Energies*, *17*(11), p.2559.

[22] https://www.kaggle.com/datasets/andrewmvd/lung-and-colon-cancer-histopathological-images

[23] Al-Jabbar, M., Alshahrani, M., Senan, E.M. and Ahmed, I.A., 2023. Histopathological Analysis for Detecting Lung and Colon Cancer Malignancies Using Hybrid Systems with Fused Features. *Bioengineering*, *10*(3), p.383.

[24] Attallah, O., Aslan, M.F. and Sabanci, K., 2022. A framework for lung and colon cancer diagnosis via lightweight deep learning models and transformation methods. *Diagnostics*, *12*(12), p.2926.